



Research article

Diffusion-weighted magnetic resonance imaging in peritoneal carcinomatosis from suspected ovarian cancer: Diagnostic performance in correlation with surgical findings



Javier Garcia Prado^{a,b,*}, Concepción González Hernando^{c,d}, David Varillas Delgado^b, Raquel Saiz Martínez^a, Priya Bhosale^e, Javier Blazquez Sanchez^a, Luis Chiva^{f,g}

^a Department of Radiology, MD Anderson Cancer Center, C/ Arturo Soria 270, 28033, Madrid, Spain

^b Facultad de Ciencias de la Salud, Universidad Francisco de Vitoria, Carretera Pozuelo-Majadahonda km 1.800 28223 Pozuelo de Alarcón (Madrid), Spain

^c Department of Radiology, Hospital Universitario Puerta de Hierro – Majadahonda, C/Manuel de Falla 1 28222, Majadahonda, Madrid, Spain

^d Universidad Autónoma de Madrid (UAM) Medicine School, C/ Arzobispo Morcillo 4, 28029, Madrid, Spain

^e Department of Radiology, MD Anderson Cancer Center, 1400 Pressler Street, FCT 15.6038, Houston, TX, 77030, United States

^f Department of Gynecology, Clínica Universitaria de Navarra, C/Marquesado de Sta. Marta, 1, 28027, Madrid, Spain

^g University of Navarra, Medicine School, Department of Gynecology -Director, C/ Iruñlarrea 1, 31008, Pamplona, Navarra, Spain

A B S T R A C T

Purpose: Ovarian cancer (OC) is the commonest cause of death by gynaecological cancer in developed countries.

Peritoneal carcinomatosis (PC) complete debulking without residual disease of > 1 cm is the best prognostic predictor in advanced OC.

PC is assessed with Computed tomography (CT). CT accuracy and cytoreduction success predictive ability are limited. PET/CT is not an imaging standard for PC.

PC shows high signal foci in Diffusion-weighted magnetic resonance imaging (DWI MRI).

We assessed the diagnostic performance (DP) and tumour burden correlation of Whole body DWI with background suppression MRI (WB-DWIBS/MRI) in PC of suspected OC using the Peritoneal Cancer Index (PCI), referring to cytoreduction surgery as the standard reference.

Method: Fifty patients with suspicion of disseminated OC underwent cytoreduction and WB-DWIBS/MRI. The PCI scores tumour burden (0–3) in 13 anatomical regions (global range of 0–39). Two radiologists (Rad1/Rad2) assessed the PCI preoperatively and with surgical findings.

We evaluated regional and global DP, the interobserver agreement (Cohen's kappa coefficient), statistical differences (McNemar test) and tumour burden (Pearson's test).

Results: 72% (36/50) were epithelial OC and 78% (39/50) achieved complete cytoreduction. Global-PCI correlation was 0.762 (Rad1) with DP: Sensitivity 0.84, specificity 0.89, accuracy 0.89, and kappa 0.41.

Average global-PCI was 7. The pelvis and right hypochondrium showed the highest positive rate and DP, while the intestinal regions presented the lowest. Previous studies reported higher sensitivity than CT or PET/CT, although only a few used the PCI.

Conclusions: WB-DWIBS/MRI is reliable to depict, quantify and to predict complete cytoreductive surgery in OC PC.

1. Introduction

Ovarian cancer (OC) is the primary cause of death by gynaecological cancer in developed countries, with an annual incidence of 3412 and a 5-year prevalence in the general population of 7939 for 2017 in Spain, similar to other industrialized countries [1,2]. The most common OC histology is epithelial type, and up to 65% of patients are diagnosed

at stages III and IV with peritoneal carcinomatosis (PC) and nodal dissemination, with high mortality [2,3].

The treatment of choice for OC is primary surgical cytoreduction followed by platinum-based adjuvant chemotherapy [4]. If there are no criteria against abdominal resection [5], achieving complete surgical debulking without residual disease > 1 cm (R0) is the best prognostic predictor in advanced OC [5,6]. Occasionally, if primary surgery cannot

Abbreviations: OC, ovarian cancer; PC, peritoneal carcinomatosis; PCI, peritoneal cancer index; CT, computed tomography; PET/CT, positron emission tomography CT with 18-fluorodeoxyglucose; HIPEC, hyperthermic intraperitoneal chemoperfusion; DWI, diffusion-weighted imaging; WB-DWIBS/MRI, whole body DWI with background suppression MRI; DP, diagnostic performance

* Corresponding author at: Department of Radiology, MD Anderson Cancer Center, C/ Arturo Soria 270, 28033, Madrid, Spain.

E-mail addresses: fjgarcia@mdanderson.es (J. Garcia Prado), cghernando@salud.madrid.org (C. González Hernando), david.varillas@ufv.es (D. Varillas Delgado), rsaiz@mdanderson.es (R. Saiz Martínez), Priya.Bhosale@mdanderson.org (P. Bhosale), jblazquez@mdanderson.es (J. Blazquez Sanchez), lchiva@unav.es (L. Chiva).

<https://doi.org/10.1016/j.ejrad.2019.108696>

Received 13 February 2019; Received in revised form 13 September 2019; Accepted 26 September 2019

0720-048X/© 2019 Elsevier B.V. All rights reserved.

be performed initially [5], interval surgery after three cycles of neoadjuvant chemotherapy may be considered. Secondary cytoreduction is performed after recurrence if there is an option for R0 debulking.

Preoperative detection of irresectable disease is crucial for the selection of surgical candidates, and the detection and location of peritoneal seeding in OC is useful in the planning of accurate surgery. Laparoscopy has been proposed as a preoperative approach to tumour evaluation using the Fagotti score [7]. This system assesses eight peritoneal structures and assigns a score of 0–2. If global scoring is ≥ 8 , then the predictive positive value (PPV) of a suboptimal surgical result is 100%. However, laparoscopy is an invasive technique, and it cannot evaluate the retroperitoneum nor the tumour posterior to the gastrosplenic ligament and in the lesser sac [8].

The peritoneal cancer index (PCI) [9] was described for PC quantification in surgical cytoreduction and hyperthermic intraperitoneal chemoperfusion (HIPEC). It is a region-wise scoring system that assesses 13 anatomic regions, each with a range of 0–3, and considers the largest lesion in each region according to the following categories: no tumour, LS0; up to 0.5 cm, LS 1; up to 5 cm, LS 2; and more than 5 cm or confluent, LS 3 (Fig. 1). The PCI is calculated through the sum of all regional scores in each patient, with a total burden range of 0–39. It is used in digestive carcinomatosis candidates for cytoreduction and HIPEC, but not as often in ovarian carcinomatosis given that the only accepted prognostic factor is complete (R0) debulking, whereas HIPEC is still under discussion for advanced OC [10].

Different imaging techniques are used in preoperative PC assessment and describe several dissemination patterns [11,12], although no imaging tool is capable of predicting the success of a R0 resection. Computed tomography (CT) is the elective technique for abdominal imaging and, when using a dedicated protocol, CT correlates well with the surgical PCI [13]. CT is recommended for staging and follow up in gynaecological malignancies by the American College of Radiology (ACR) and National Comprehensive Cancer Network (NCCN) guidelines. The accuracy of CT for PC in OC and its capability for predicting the success of cytoreductive surgery is limited, although when evaluated with CA-125 levels it may predict prognosis [14,15]. Positron emission tomography CT with 18-fluorodeoxyglucose (PET/CT) can be considered for systemic evaluation of gynaecological malignancies, although it is not yet established as a reference standard for PC depiction

[16]. Conventional MRI is useful in peritoneal carcinomatosis [17], however its diagnostic performance (DP) is inferior to PET/CT [18,19] and similar to CT [20]. Diffusion-weighted imaging (DWI) is obtained using high-energy short-time MR radiofrequency pulses, where the *b* value expresses the strength of potentiation in diffusion. Using high *b* values ($b \text{ max} \geq 1000$), DWI provides a very high signal intensity of structures with water movement restriction and almost no signal from other anatomical structures. Dynamic contrast-enhanced imaging and DWI improve the capability of tumour pelvic recurrence characterisation [21], and the addition of high *b* DWI to routine MRI raises the DP for peritoneal metastases [22–25]. Finally, whole body DWI with background suppression MRI (WB-DWIBS/MRI) combines high *b* DWI with conventional imaging of the entire body for anatomical referencing and characterisation of findings [26].

This study aimed to assess the DP and tumour burden correlation of WB-DWIBS/MRI in PC from suspected OC using the PCI, referring to cytoreduction surgery as the standard reference.

2. Material and methods

2.1. Study design

This is an observational, prospective, single-institution, non-comparative, DP study of WBMRI/DWIBS versus the pathologically-proven surgical standard of reference. Institutional review board approval was obtained, and all patients signed written informed consent.

2.2. Study population

Inclusion criteria included suspected diagnosis of a primary or recurrent ovarian carcinoma according to raised CA-125 levels and imaging findings. Exclusion criteria were claustrophobia, known renal impairment (creatinine $> 1.5 \text{ mg/dl}$ or glomerular filtration rate $< 60 \text{ ml/min/1.73m}^2$), contraindications to hyoscine butyl-bromide (allergies, glaucoma, history of bowel obstruction, or urinary retention), non-operable patients, and non-resectable disease [5,8]. Patients considered for interval debulking surgery were disregarded for this study.

From June 2014 to January 2017, 217 consecutive patients presented at our institution and were evaluated at interdisciplinary

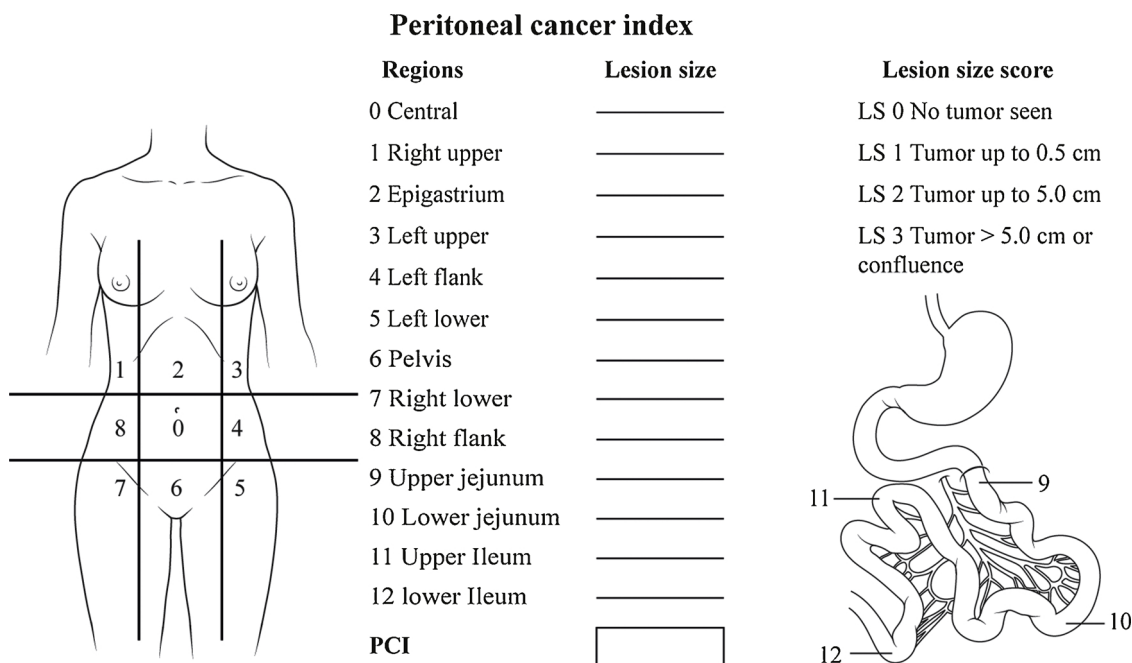


Fig. 1. Peritoneal cancer index (PCI) diagram showing the 13 evaluated regions and the possible tumour burden (0–3) according to implant size.

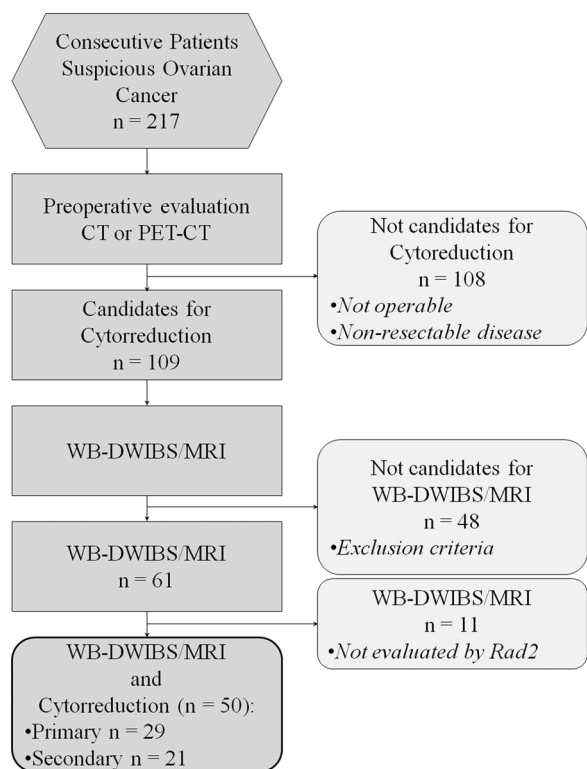


Fig. 2. Flowchart showing the sample selection criteria for the study.

meetings. Of these, 108 were considered for initial chemotherapy and 109 were candidates for cytoreduction and were offered a WBMRI/DWIBS examination. Sixty-one patients met all the inclusion criteria (Fig. 2); of these, 11 patients were evaluated by Rad1 and underwent surgery with no evaluation by Rad2, thus they were excluded from the study to avoid any information bias. In total, 50 patients were finally considered for the study. Any finding on WBMRI/DWIBS beyond the surgical field that would preclude surgery was studied with other techniques and biopsied when possible.

Table 1

Sequence protocol of WB-DWIBS/MRI. DWIBS, diffusion-weighted imaging with background suppression; 3DT1GE, 3D volumetric gradient echo T1; THRIVE, T1-weighted high resolution isotropic volume examination; SPAIR, spectrally adiabatic inversion recovery; mDIXON, multi-echo 2-point DIXON.

| Primary Acquisition | DWIBS | T2TSE | 3DT1GE | |
|-------------------------------------|----------------------------------------------|-----------------------------------|------------------------------------------|-----------------|
| Orientation: | Coronal | Axial, coronal | Axial, coronal | Axial |
| Coverage: | Head – mid thigh | Head – mid thigh | Abdomen – pelvis | Chest |
| Repetition time (TR): | 4736 | 1000 | 5.9 | 3.7 |
| Echo Time (TE): | 78 | 80 | 1.8 | 1.76 |
| Flip angle | | | 15° | 10° |
| Number of signal Average (NSA): | 4 | 1 | 1 | 1 |
| FOV (RL × AP × CC) (mm): | 450 × 230 × 300 | 498 × 230 × 400 | 400 × 352 × 230 | 400 × 359 × 230 |
| Station Number: | 3 | 4 | 2 | 1 |
| Slice Thickness (ST) (mm): | 6 | 6 | 4 | 4 |
| Slice Number (SN) Coronal: | 40 | 35 | 120 | |
| Slice Number (SN) Axial: | | 140 | 120 | 115 |
| Slice Spacing (mm): | 0 | 1 | 0 | 0 |
| Acquired voxel size (RL × AP × CC): | 3.5 × 3.5 | 2 × 1.6 | 2 × 2 × 4 | 2.56 × 2.56 × 4 |
| Reconstructed voxel size : | 1.76 | 1.04 | 1 × 1 × 2 | 1 × 1 × 2 |
| Respiration | Free | Triggered | Breathhold | Breathhold |
| Parallel imaging factor (SENSE) | 4 | 2 | 2 × 1.3 | 2 × 1.3 |
| Fat suppression | | | SPAIR (mDIXON) | SPAIR (eTHRIVE) |
| b values (s/mm ²) | 0-1000 | | | |
| Derived Images | | Color fusion (DW overlay) Coronal | Color fusion (DW overlay) Axial, coronal | |
| | MIP Axial, sagittal 3D Volumetric Coronal | | | |

2.3. Imaging protocol

Patients drank 1 L of pure pineapple juice 2 h before imaging as a negative oral contrast agent. We injected 20 mg of hyoscine butylbromide diluted in 100 ml saline solution; 50 ml was administered at the beginning of the examination and the other 50 ml before the DWIBS sequence. Intravenous contrast gadobutrol at 1 mmol/ml (0.2 ml/kg weight) was given at an injection rate of 2 ml/s (MEDRAD® Spectris Solaris EP Injection System, Bayer AG Leverkusen, Germany).

Imaging was performed on a 1.5 T system (Ingenia, Philips Healthcare, Best, Netherlands) (Table 1) with head/neck and two body phased-array coils for anatomical coverage from the head to the mid thighs [25,26].

Coronal and axial single-shot T2-weighted turbo spin echo (T2TSE) and volumetric 3DT1-weighted fat sat gradient-echo (3DT1GE) for anatomical evaluation and DWIBS imaging (b-values: 0 and 1000s/mm²) were obtained in the coronal plane.

In a dedicated MR workstation (IntelliSpace Portal Version 606.20039, Philips Medical Systems Nederland B.V.), we obtained re-formatted maximum intensity projection (MIP) images in the axial and sagittal planes, colour-derived maps using T2TSE and 3DT1GE as a reference layer, and MIP-DWIBS as a colour functional overlay (alpha blending, 50%).

2.4. Imaging analysis

Two radiologists (Rad1 and Rad2, who had 10 and 5 years of experience in abdominal imaging, respectively) read the same 50 examinations, and were both blinded to medical history and the other radiologist’s findings. They used the PCI (Fig. 1) [9] to assess regional DP in the 50 cases.

CT or PET/CT were not evaluated given that they were performed at external institutions with wide technical variations, therefore comparisons were not possible. We considered DWIBS primarily for tumour detection and the findings were correlated with T2TSE and 3DT1GE sequences for anatomical location.

A positive finding was considered for any size of nodular, plaque, or linear intrabdominal high signal foci on DW and was measured (0–3) for every region (13) in each patient, based on the PCI. If a nodule was detected in conventional images but showed no signal in DWI, it was

Table 2
Clinical characteristics and outcome in included patients.

| | | | |
|-----------------------------|----------------------------------------|-------------------|------------|
| Age *(years) | mean, (sd) | 56.00 | (12.69) |
| Time to surgery (days) | median, (range) | 12 | (37) |
| CA-125 prior surgery (U/ml) | Median,(range) | 167.5 | (11,760.8) |
| Primary site | | Total (n = 50) | |
| | Ovary | 38 | |
| | Fallopian tube | 1 | |
| | Uterus | 2 | |
| | Cervix | 3 | |
| | Other non-malignant Gynecologic | 3 | |
| | Other malignant non-Gynecologic | 3 | |
| Disease stage | FIGO | Total (n = 50) | |
| | IA | 8 | |
| | IB1 | 1 | |
| | IC1 | 1 | |
| | IIA | 1 | |
| | IIB | 1 | |
| | IIIA1 | 1 | |
| | IIIC | 9 | |
| | IV | 2 | |
| | N/A | 5 | |
| | Recurrent | 21 | |
| Histology | | Total (n = 50) | |
| | Serous adenocarcinoma | 28 | |
| | Clear cell | 4 | |
| | Mixed Müllerian Malignant Tumor (MMMT) | 3 | |
| | Serous cystadenoma | 2 | |
| | Endometriosis | 2 | |
| | Borderline Tumor | 2 | |
| | Endocervical Adenocarcinoma | 1 | |
| | Breast Adenocarcinoma | 1 | |
| | Biliary adenocarcinoma | 1 | |
| | Endometrioid Adenocarcinoma | 2 | |
| | Adenosarcoma | 1 | |
| | Leiomyoma | 1 | |
| | Gastro Intestinal Stromal Tumor (GIST) | 1 | |
| | Borderline Mucinous Tumor | 1 | |
| Surgical outcome | | Total (n = 50) | |
| | Microscopic (Complete) | 39 | |
| | Macroscopic < 1 cm (Optimal) | 7 | |
| | Macroscopic > 1 cm (Suboptimal) | 4 | |

considered positive and was documented using the PCI.

Peritoneal surface contrast enhancement, ascites, or adhesions were not considered as peritoneal tumour. We did not evaluate the apparent diffusion coefficient (ADC) given the small size of some implants.

2.5. Standard of reference

OC treatment-naïve patients with indications for surgical resection were considered for primary cytoreduction, and those who had prior surgery were considered for non-primary cytoreduction.

Operability was considered according to clinical status and anatomical resectability criteria that were evaluated with the initial imaging techniques. PCI calculated prior to surgery was not considered for the surgical indication.

All the patients were operated upon by the same gynaecological surgeon and general surgeon. The same two pathologists evaluated all samples. Each of the pathologists and surgeons had more than 15 years of experience each in gynaecological oncology.

Regions were assessed during surgery according to the PCI system and specimens were labelled for subsequent pathological confirmation. Any finding on WBMRI/DWIBS beyond the surgical field that would preclude surgery was studied with other techniques and biopsied whenever possible.

2.6. Statistical analysis

SPSS v21.0 software (IBM) was used with *P*-values of < 0.05 indicating statistical significance. WBMRI/DWIBS findings were compared with surgery to obtain the sensitivity, specificity, positive predictive value (PPV), negative predictive value, and accuracy. Statistical differences between both techniques were calculated with the two-tailed McNemar test and Bonferroni correction was used to avoid biases.

Cohen's kappa coefficient was used to evaluate interobserver agreement ($\kappa < 0.2$, slight; < 0.4 , fair; < 0.6 , moderate; < 0.8 , substantial; > 0.8 perfect). Surgical and preoperative global PCI was assessed with Pearson's correlation coefficient test.

3. Results

3.1. Clinical results

A total of 50 patients were selected for this study. Peritoneal seeding in 13 PCI regions was pathologically confirmed after surgery (Fig. 1). Table 2 shows the clinical outcome. Surgery was delayed in some patients due to acute comorbidities (acute infections, renal impairment and others).

Almost all the patients (94%, 47/50) presented with primary gynaecological disease; 88% (44/50) were primary gynaecological malignancies and 76% (38/50) were of ovarian origin, while the histology was epithelial type in 72% (36/50).

3.2. Imaging results

3.2.1. Global evaluation

Fig. 3 presents the frequency of disease detected in each region and Table 3 details the DP of WBMRI/DWIBS as assessed by Rad1 and Rad2.

The global average surgical PCI was 7.42 ± 5.675 and 7.08 ± 5.865 for Rad1 and for Rad2, respectively. The tumour burden, as assessed by Pearson's correlation coefficient, was 0.762 ($p < 0.001$) for Rad1 and 0.642 ($p < 0.001$) for Rad2 (Fig. 4).

Overall positive scoring (score values 1–3) for surgical findings, Rad1, and Rad2 were 28.46%, 30.77%, and 24.15%, respectively (Fig. 5).

We also explored the distribution of the total PCI for both observers and surgery (Fig. 6) based on cytoreduction results, and we found that lower initial tumour burden was followed by a higher frequency of complete cytoreduction ($p < 0.05$).

Interobserver agreement was globally fair to moderate, although it was moderate to substantial in six out of 13 regions evaluated.

3.2.2. Regional evaluation

The pelvis presented the highest number of positives for both observers and surgery with high sensitivity but moderate specificity. The central region had the second highest positive rate, with moderate sensitivity and high specificity for both observers.

The bowel loops showed a low detection rate, although they presented a good diagnostic performance.

Accuracy was over 0.86 in all regions for Rad1 and above 0.8 in 6/13 regions for Rad2, and global accuracy was 0.89 and 0.8, respectively.

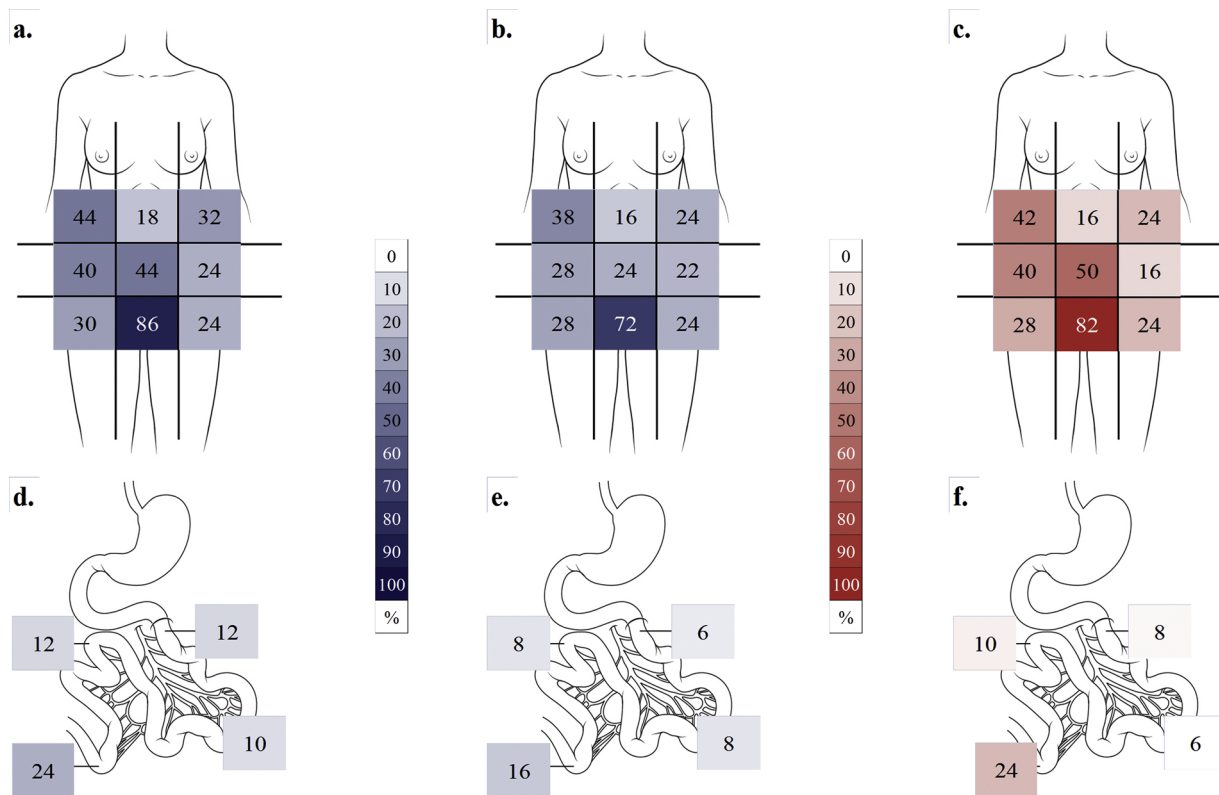


Fig. 3. Percentage of positives detected in the different peritoneal regions using the PCI system, as evaluated by observers Rad1 (a, d) and Rad2 (b, e) using WB-DWIBS/MRI compared with surgery (c, f).

Table 3
Global and regional DP of WB-DWIBS/MRI for both observers (Rad1 and Rad2) and surgery.

| Peritoneal cavity | Observer | TP | TN | FP | FN | Sensitivity | Specificity | PPV | NPV | Accuracy | Kappa |
|-------------------|-------------|------------|------------|-----------|-----------|---------------------|------------------|------------------|---------------------|---------------------|-------------|
| 0 Central | Rad1 | 20 | 23 | 2 | 5 | 0.8 | 0.92 | 0.91 | 0.82 | 0.86 | 0.41 |
| | Rad2 | 11 | 24 | 1 | 14 | 0.44 | 0.96 | 0.92 | 0.63 | 0.7 | |
| 1 Right upper | Rad1 | 18 | 25 | 4 | 3 | 0.86 | 0.86 | 0.82 | 0.89 | 0.86 | 0.63 |
| | Rad2 | 14 | 24 | 5 | 7 | 0.67 | 0.83 | 0.74 | 0.77 | 0.76 | |
| 2 Epigastrium | Rad1 | 6 | 39 | 3 | 2 | 0.75 | 0.93 | 0.67 | 0.95 | 0.9 | 0.22 |
| | Rad2 | 2 | 36 | 6 | 6 | 0.25 | 0.86 | 0.25 | 0.86 | 0.76 | |
| 3 Left upper | Rad1 | 11 | 33 | 5 | 1 | 0.92 | 0.87 | 0.69 | 0.97 | 0.88 | 0.8 |
| | Rad2 | 9 | 35 | 3 | 3 | 0.75 | 0.92 | 0.75 | 0.92 | 0.88 | |
| 4 Left flank | Rad1 | 7 | 37 | 5 | 1 | 0.88 | 0.88 | 0.58 | 0.97 | 0.88 | 0.61 |
| | Rad2 | 5 | 36 | 6 | 3 | 0.63 | 0.86 | 0.45 | 0.92 | 0.82 | |
| 5 Left lower | Rad1 | 6 | 32 | 6 | 6 | 0.5 | 0.84 | 0.5 | 0.84 | 0.76 | 0.34 |
| | Rad2 | 4 | 30 | 8 | 8 | 0.33 | 0.79 | 0.33 | 0.79 | 0.68 | |
| 6 Pelvis | Rad1 | 40 | 6 | 3 | 1 | 0.98 | 0.67 | 0.93 | 0.86 | 0.92 | 0.51 |
| | Rad2 | 32 | 5 | 4 | 9 | 0.78 | 0.56 | 0.89 | 0.36 | 0.74 | |
| 7 Right lower | Rad1 | 11 | 32 | 4 | 3 | 0.79 | 0.89 | 0.73 | 0.91 | 0.86 | 0.27 |
| | Rad2 | 8 | 30 | 6 | 6 | 0.57 | 0.83 | 0.57 | 0.83 | 0.76 | |
| 8 Right flank | Rad1 | 17 | 27 | 3 | 3 | 0.85 | 0.9 | 0.85 | 0.9 | 0.88 | 0.47 |
| | Rad2 | 11 | 27 | 3 | 9 | 0.55 | 0.9 | 0.79 | 0.75 | 0.76 | |
| 9 Upper jejunum | Rad1 | 4 | 44 | 2 | 0 | 1 | 0.96 | 0.67 | 1 | 0.96 | 0.4 |
| | Rad2 | 2 | 45 | 1 | 2 | 0.5 | 0.98 | 0.67 | 0.96 | 0.94 | |
| 10 Lower jejunum | Rad1 | 3 | 45 | 2 | 0 | 1 | 0.96 | 0.6 | 1 | 0.96 | 0.15 |
| | Rad2 | 1 | 44 | 3 | 2 | 0.33 | 0.94 | 0.25 | 0.96 | 0.9 | |
| 11 Upper Ileum | Rad1 | 4 | 43 | 2 | 1 | 0.8 | 0.96 | 0.67 | 0.98 | 0.94 | 0.12 |
| | Rad2 | 2 | 43 | 2 | 3 | 0.4 | 0.96 | 0.5 | 0.93 | 0.9 | |
| 12 Lower Ileum | Rad1 | 9 | 35 | 3 | 3 | 0.75 | 0.92 | 0.75 | 0.92 | 0.88 | 0.38 |
| | Rad2 | 5 | 35 | 3 | 7 | 0.42 | 0.92 | 0.63 | 0.83 | 0.8 | |
| Summary | Rad1 | 156 | 421 | 44 | 29 | 0.84 | 0.89 | 0.72 | 0.92 | 0.89 | 0.41 |
| | Rad2 | 106 | 414 | 51 | 79 | 0.51 | 0.87 | 0.6 | 0.81 | 0.8 | |
| | | | | | | p < 0.001 | p = 0.151 | p = 0.006 | p < 0.001 | p < 0.001 | |

4. Discussion

This prospective study evaluated DP and tumour burden quantification using WB-DWIBS/MRI in suspected ovarian PC, comparing the

imaging PCI with the surgical PCI in patients undergoing primary or secondary cytoreduction. Patients who received interval debulking surgery after three cycles of chemotherapy were excluded from the study, given that tumour necrosis and bleeding might be a source of

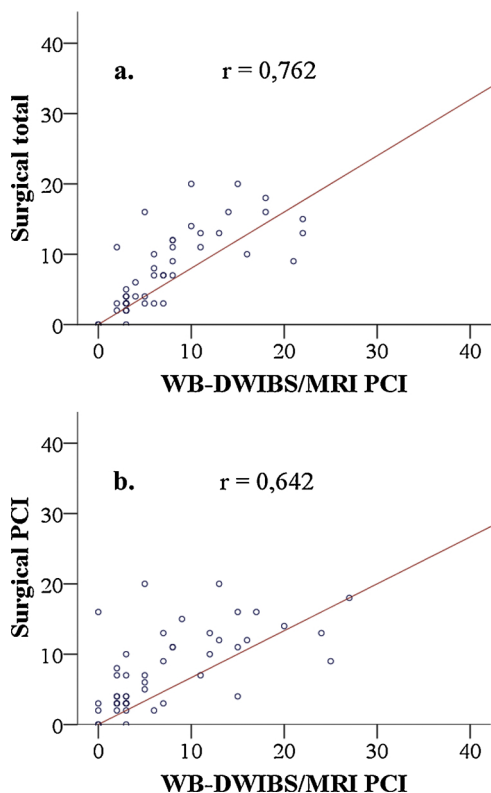


Fig. 4. Total surgical (vertical axis) and total WB-DWIBS/MRI (horizontal axis) PCI correlation for Rad1 (a) and Rad2 (b).

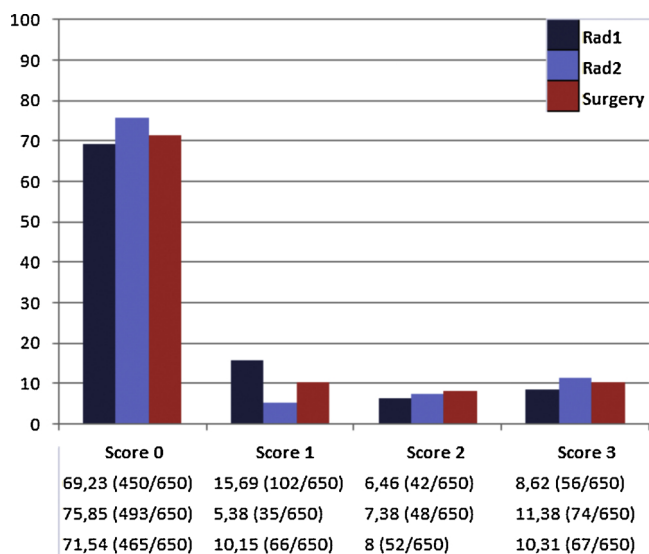


Fig. 5. Bar chart showing overall PCI score distribution of 650 (13 regions × 50 patients) observations. The results are presented in percentages and ratios in brackets.

false positives [28].

Secondary cytoreduction is a different clinical situation, in that recurrence in patients some considerable time after their primary surgery can be considered as new disease.

We adopted the PCI [9] as a reproducible means for determining PC distribution and tumour burden quantification for different imaging techniques [13,15,17,29–34] and surgical findings; others evaluated WB-MRI/DWIBS for regional ovarian carcinomatosis [25,27,35–37] in non-PCI anatomical compartments. Thus, local assessment and comparisons are difficult given the variations in classifications, although

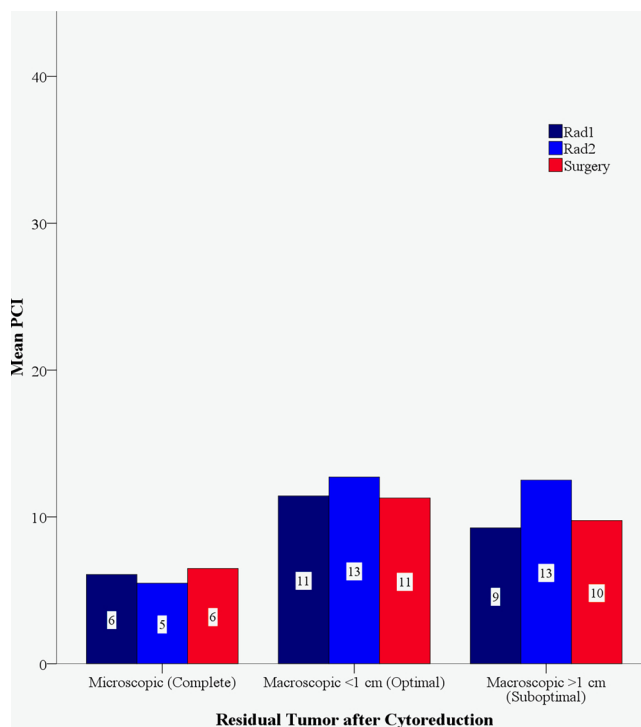


Fig. 6. Global PCI tumour burden evaluated by Rad1, Rad2, and surgery according to cytoreduction results.

global evaluation can be useful.

In the current study, global tumour burden was low (average PCI, 7) and most of the regions showed no peritoneal implants because many of the patients with high tumour burden did not fulfil the operability or resectability criteria, and therefore were not eligible for this study.

We found a significant correlation between the peritoneal tumour burden of MRI compared with surgery that was better than that reported for PET/CT or CT [16].

The pelvis followed by right hypochondrium showed the highest positive rate and diagnostic performance. The first because it is the site of the primary tumour and peritoneal implant deposits due to the effect of gravity, and the second because of the high contrast of the tumour with the liver surface (Fig. 7), whose signal is almost null in DWIBS compared with the lack of density differences in CT or PET/CT.

The intestinal regions presented the lowest positive rate because massive infiltration may preclude surgical resection if it indicates multiple anastomosis. The central zone showed a variable positive rate, partly because mesentery root infiltration may also contraindicate surgery and because omental infiltration is difficult to assign in one of these compartments. Moreover, assignment of a lesion to one or another compartment was sometimes challenging.

WB-DWIBS/MRI global and regional accuracies were statistically significant with good values, although there were regional variations.

Global PCI distribution (Fig. 6) suggested that WB-DWIBS/MRI might predict the cyto reduction result, with higher residual tumour when a higher PCI was calculated.

Our results are in line with previous studies (Table 4). To the best of our knowledge, only one previous study evaluated ovarian carcinomatosis with WB-DWIBS/MRI using PCI [32] with higher sensitivity when compared with CT and PET/CT; however, this was only conducted in 15 patients. Other studies assessing gynaecological cancer with DWIBS reported similar results, with a better DP than CT, although with variable designs, sample sizes, and different regional evaluation than the PCI [27,35–38,42].

Our DP in region 5 overlaps with that recently described for splenic infiltration [39] both for CT and MRI. The findings can be partially

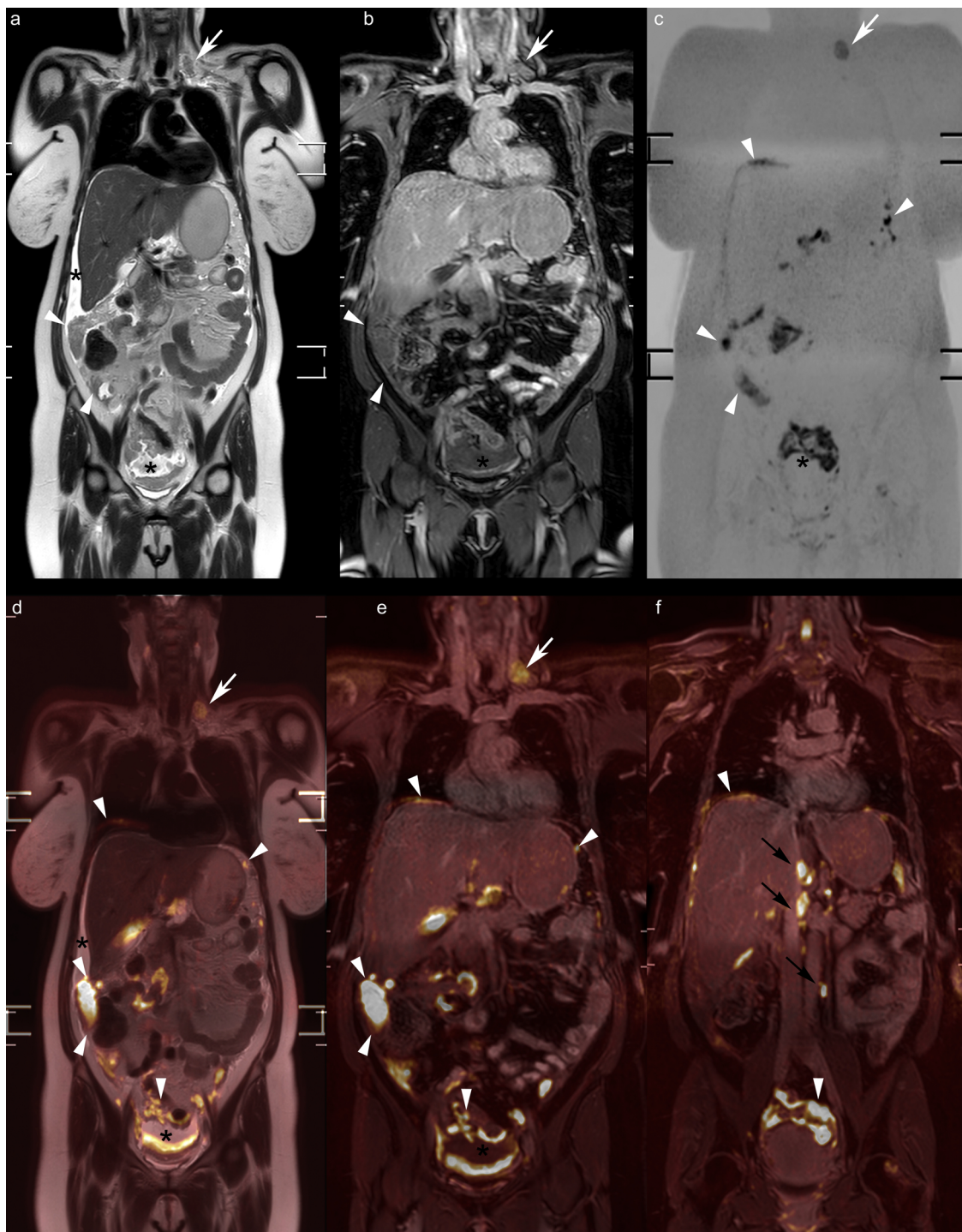


Fig. 7. Coronal native images weighted in T2TSE (a), 3DGET1 (b), and DWIBS (c) and red-scale DWIBS-fused imaging with T2 (d) and 3DGET1 (e) in the same planes as above and in the para-aortic plane (f). Asterisks show ascites in both flanks and pelvis. Peritoneal carcinomatosis (white arrowheads) is shown in flanks, greater omentum, and subdiaphragmatic and perihepatic spaces, left hypochondrium, and pelvis surrounding ascites. Para-aortic and pericaval lymph nodes (black arrows) and supraclavicular node (white arrow) are depicted.

explained by the physiologically high DWI signal of the spleen that may make tumour detection. Miliary carcinomatosis and different critical peritoneal regions must be evaluated.

When compared with PET/CT, WB-DWIBS/MRI shows better [27,38] or at least similar [24,32] DP for PC. Some studies reported better results for PET/CT, though MR did not combine DWI sequences [18], nor were they considered in an initial meta-analysis [19]. However, a more recent study reported a better performance for WB-

DWIBS/MRI than PET/CT [40].

Our regional sensitivities were very close to those previously reported [22,31,32] when evaluating WB-DWIBS/MRI with the PCI for local diagnostic performance, although with higher specificities in almost every region, probably because the use of higher *b* values (*b*1000), with the exception of the pelvis, which also showed better sensitivity.

One major limitation is that 11 patients had no OC histologies. They were included in the study given its prospective design in order to avoid

Table 4

Diagnostic performances reported for computed tomography (CT), positron emission tomography CT(PET/CT) and magnetic resonance with and without diffusion weighted sequences (DW/ No DW) in peritoneal carcinomatosis using peritoneal cancer index (PCI) or other classifications (NonPCI). Carcinomatosis are of ovarian origin (Ovarian); gynaecologic, not specifically ovarian (Gynaecologic) or a different origin (Other). Sn, sensitivity; Sp, specificity; Acc, accuracy; the values are provided in percentage. (*) are meta-analysis.

| Author | Year | Sample | Origin | Peritoneal Evaluation | MRI Technique | CT | | | PET/CT | | | MRI | | | |
|--------|-------------|--------|--------|-----------------------|---------------|--------|----------|----------|--------|-------|-------|-----|--------|----------|------|
| | | | | | | Sn | Sp | Acc | Sn | Sp | Acc | Sn | Sp | Acc | |
| [30] | Low | 2015 | 22 | Other | PCI | DW | 55 | 86 | 63 | - | - | - | 95 | 70 | 88 |
| [32] | Schmidt | 2015 | 15 | Ovarian | PCI | DW | 96 | 92 | | 95 | 96 | 96 | 98 | 84 | 93 |
| [33] | Low | 2012 | 33 | Other | PCI | DW | 88 | 74 | 84 | - | - | - | - | - | - |
| [13] | Mazzei | 2013 | 43 | Ovarian | PCI | No MRI | 100 | 40 | 93 | - | - | - | - | - | - |
| [31] | De Iaco | 2011 | 40 | Ovarian | PCI | No MRI | - | - | - | 78,9 | 68,4 | - | - | - | - |
| [37] | Fehniger | 2016 | 27 | Gynaecologic | Non PCI | DW | 7,7-95,2 | 33,3-100 | - | - | - | - | 0-94,1 | 44,4-100 | - |
| [38] | Michielsen | 2017 | 161 | Ovarian | Non PCI | DW | 66 | 77,3 | 71,3 | - | - | - | 94 | 97,7 | 95,7 |
| [35] | Michielsen | 2016 | 51 | Ovarian | Non PCI | DW | 0-83 | 92-100 | - | - | - | - | 52-100 | 33-100 | - |
| [27] | Michielsen | 2014 | 32 | Ovarian | Non PCI | DW | 65 | 82 | 75 | 52 | 85 | 71 | 91 | 91 | 91 |
| [23] | Bozkurt | 2011 | 19 | Other | Non PCI | DW | - | - | - | - | - | - | 83 | 94 | 86 |
| [36] | Espada | 2013 | 36 | Ovarian | Non PCI | DW | - | - | - | - | - | - | 50-100 | 83,3-100 | - |
| [22] | Low | 2009 | 34 | Other | Non PCI | DW | - | - | - | - | - | - | 71 | 90 | 81 |
| [40] | Li (*) | 2014 | 1067 | Other | Non PCI | DW | - | - | - | 89,5 | 97,5 | - | 89,7 | 85,4 | - |
| [16] | Lopez-Lopez | 2016 | 59 | Ovarian | Non PCI | No MRI | 35 | 98 | - | 24 | 93 | - | - | - | - |
| [19] | Gu (*) | 2009 | - | Ovarian | Non PCI | No DW | 79 | 84 | - | 91 | 88 | - | 75 | 78 | - |
| [17] | Klumpp | 2013 | 15 | Other | Non PCI | No DW | - | - | - | 92-93 | 94-96 | - | 87 | 86-92 | - |
| [41] | Kubik-Huch | 2000 | 19 | Ovarian | Non PCI | No DW | 100 | 67 | 86 | 100 | 67 | 86 | 100 | 100 | 100 |

any information bias. All patients fulfilled inclusion criteria. Some of them mimicked OC (leiomyomas) and other may associate OC (endometriosis). One patient with prior breast cancer presented with PC and negative bone biopsies so peritoneal biopsies were collected to exclude OC given their clinical association, and PCI was also surgically calculated.

Nevertheless, we have also calculated specific PCI and DP for those PC of pathologically proven OC origin (n = 39). We found that global interobserver agreement was slightly better (kappa 0.53) and global PCI was also slightly higher (PCI 8) with no further differences with the original sample (Supplementary Tables 1 and 2).

Another limitation is that this is a single institutional study. There may be an occult selection bias because the patients selected for the study were also candidates for cytoreduction. Therefore, the resectability itself and the areas that may contraindicate resectability might be under evaluated.

Although patients undergoing interval-debulking surgery were excluded, more than half of the study population consisted of post-operative patients, and therefore DP may have been affected. T2 shine-through may be a source of false positive findings in DWIBS sequences, especially in dense fluids such as blood, mucin, or coagulative necrosis that maintain a hyperintense signal in high b DWIBS imaging [28]. However, these can be confirmed with other sequences (T2- or T1-contrast enhanced). Another major limitation is that we did not directly compare WB-DWIBS/MRI with other imaging techniques such as CT or PET/CT. This was because the patients were referred by different institutions with various initial modalities and wide variations in imaging protocols.

Nonetheless, this is a prospective study of a moderately large and very homogeneous sample population in which almost all patients were diagnosed with OC. We present a quantitative approach of our imaging findings related to surgery.

Even though it is beyond the scope of this study, WB-DWIBS/MRI can evaluate nodal and supradiaphragmatic dissemination. Given that ADC was not evaluated, further research may be needed to establish a cut-off point for DW signal intensity, similar to the standard uptake value (SUV) for PET/CT.

In conclusion, WB-DWIBS/MRI is a reliable imaging technique that is useful in preoperatively quantifying and depicting PC in OC to achieve complete cytoreductive surgery.

Declaration of Competing Interest

The authors declare that they have no known competing financial interests or personal relationships that could have appeared to influence the work reported in this paper.

Acknowledgements

We thank H. Nikki March, PhD, from Edanz Group (www.edanzediting.com/ac) for editing a draft of this manuscript and David Gutiérrez Pérez, BS in Mathematics, for the initial design of this study.

Appendix A. Supplementary data

Supplementary material related to this article can be found, in the online version, at doi:<https://doi.org/10.1016/j.ejrad.2019.108696>.

References

- https://seom.org/seomcms/images/stories/recursos/Las_Cifras_del_cancer_en_Espana2018.pdf.
- L.A. Torre, B. Trabert, C.E. DeSantis, K.D. Miller, G. Samimi, C.D. Runowicz, M.M. Gaudet, A. Jemal, R.L. Siegel, Ovarian cancer statistics, 2018, CA: Cancer J. Clin. 68 (2018) 284–296, <https://doi.org/10.3322/caac.21456>.
- Kurman, Robert J., 2014. International Agency for Research on Cancer, World Health Organization, WHO classification of tumours of female reproductive organs, Lyon: International Agency for Research on Cancer, France, 2014.
- T. Thigpen, The if and when of surgical debulking for ovarian carcinoma, N. Engl. J. Med. 351 (2004) 2544–2546, <https://doi.org/10.1056/NEJMe048292>.
- D. Querleu, F. Planchamp, L. Chiva, C. Fotopoulou, D. Barton, D. Cibula, G. Aletti, S. Carinelli, C. Creutzberg, B. Davidson, P. Harter, L. Lundvall, C. Marth, P. Morice, A. Rafii, I. Ray-Coquard, A. Rockall, C. Sessa, A. van der Zee, I. Vergote, A. duBois, European Society of Gynaecological Oncology (ESGO) guidelines for ovarian cancer surgery, Int. J. Gynecol. Cancer 27 (2017) 1534–1542, <https://doi.org/10.1097/IGC.0000000000001041>.
- I. Vergote, C.G. Tropé, F. Amant, G.B. Kristensen, T. Ehlen, N. Johnson, R.H. Verheijen, M.E. van der Burg, A.J. Lacave, P.B. Panici, et al., Neoadjuvant chemotherapy or primary surgery in stage IIIC or IV ovarian cancer, N. Engl. J. Med. 363 (2010) 943–953.
- A. Fagotti, G. Ferrandina, F. Fanfani, G. Garganese, G. Vizzielli, V. Carone, M.G. Salerno, G. Scambia, Prospective validation of a laparoscopic predictive model for optimal cytoreduction in advanced ovarian carcinoma, Am. J. Obstet. Gynecol. 199 (2008) 642, <https://doi.org/10.1016/j.ajog.2008.06.052> e1–6.
- S. Nougaret, H.C. Addley, P.E. Colombo, S. Fujii, S.S. Al Sharif, S.H. Tirumani, K. Jardon, E. Sala, C. Reinhold, Ovarian carcinomatosis: how the radiologist can help plan the surgical approach, Radiographics 32 (2012) 1775–1800, <https://doi.org/10.1148/rg.326125511>.
- P.H. Sugarbaker, Review of a personal experience in the management of

- carcinomatosis and sarcomatosis, *Jpn. J. Clin. Oncol.* 31 (2001) 573–583.
- [10] L.M. Chiva, A. Gonzalez-Martin, A critical appraisal of hyperthermic intraperitoneal chemotherapy (HIPEC) in the treatment of advanced and recurrent ovarian cancer, *Gynecol. Oncol.* 136 (2015) 130–135, <https://doi.org/10.1016/j.ygyno.2014.11.072>.
- [11] S. González-Moreno, L. González-Bayón, G. Ortega-Pérez, C. González-Hernando, Imaging of peritoneal carcinomatosis, *Cancer J.* 15 (2009) 184–189, <https://doi.org/10.1097/PPO.0b013e3181a58ec3>.
- [12] F. Iafrate, M. Ciolina, P. Sarmmartino, P. Baldassari, M. Rengo, P. Lucchesi, S. Sibio, F. Accarpio, A. Di Giorgio, A. Laghi, Peritoneal carcinomatosis: imaging with 64-MDCT and 3T MRI with diffusion-weighted imaging, *Abdom. Imaging* 37 (2012) 616–627, <https://doi.org/10.1007/s00261-011-9804-z>.
- [13] M.A. Mazzei, L. Khader, A. Cirigliano, N. Cioffi Squitieri, S. Guerrini, B. Forzoni, D. Marrelli, F. Roviello, F.G. Mazzei, L. Volterrani, Accuracy of MDCT in the pre-operative definition of Peritoneal Cancer Index (PCI) in patients with advanced ovarian cancer who underwent peritonectomy and hyperthermic intraperitoneal chemotherapy (HIPEC), *Abdom. Imaging* 38 (2013) 1422–1430, <https://doi.org/10.1007/s00261-013-0013-9>.
- [14] R.S. Suidan, P.T. Ramirez, D.M. Sarasohn, J.B. Teitcher, S. Mironov, R.B. Iyer, Q. Zhou, A. Iasonos, H. Paul, M. Hosaka, C.A. Aghajanian, M.M. Leitaog Jr., G.J. Gardner, N.R. Abu-Rustum, Y. Sonoda, D.A. Levine, H. Hricak, D.S. Chi, A multi-center prospective trial evaluating the ability of preoperative computed tomography scan and serum CA-125 to predict suboptimal cytoreduction at primary debulking surgery for advanced ovarian, fallopian tube, and peritoneal cancer, *Gynecologic Oncology*. 134 (n.d.) 455–461, doi:10.1016/j.ygyno.2014.07.002.
- [15] D. Diaz-Gil, F.J. Fintelmann, S. Molaei, A. Elmi, S.S. Hedgire, M.G. Harisinghani, Prediction of 5-year survival in advanced-stage ovarian cancer patients based on computed tomography peritoneal carcinomatosis index, *Abdom. Radiol. (N. Y.)* 41 (2016) 2196–2202, <https://doi.org/10.1007/s00261-016-0817-5>.
- [16] V. Lopez-Lopez, P.A. Cascales-Campos, J. Gil, L. Frutos, R.J. Andrade, M. Fuster-Quionero, E. Feliciangeli, E. Gil, P. Parrilla, Use of (18)F-FDG PET/CT in the preoperative evaluation of patients diagnosed with peritoneal carcinomatosis of ovarian origin, candidates to cytoreduction and hipec. A pending issue, *Eur. J. Radiol.* 85 (2016) 1824–1828, <https://doi.org/10.1016/j.ejrad.2016.08.006>.
- [17] B. Klumpp, P. Aschoff, N. Schwenzer, I. Koenigsrainer, S. Beckert, C.D. Claussen, S. Miller, A. Koenigsrainer, C. Pfannenberger, Correlation of preoperative magnetic resonance imaging of peritoneal carcinomatosis and clinical outcome after peritonectomy and HIPEC after 3 years of follow-up: preliminary results, *Cancer Imaging* 13 (2013) 540–547, <https://doi.org/10.1102/1470-7330.2013.0044>.
- [18] B.D. Klumpp, N. Schwenzer, P. Aschoff, S. Miller, U. Kramer, C.D. Claussen, B. Bruecher, A. Koenigsrainer, C. Pfannenberger, Preoperative assessment of peritoneal carcinomatosis: intraindividual comparison of 18F-FDG PET/CT and MRI, *Abdom. Imaging* 38 (2013) 64–71, <https://doi.org/10.1007/s00261-012-9881-7>.
- [19] P. Gu, L.-L. Pan, S.-Q. Wu, L. Sun, G. Huang, CA-125, PET alone, PET-CT, CT and MRI in diagnosing recurrent ovarian carcinoma: a systematic review and meta-analysis, *Eur. J. Radiol.* 71 (2009) 164–174, <https://doi.org/10.1016/j.ejrad.2008.02.019>.
- [20] C.M.C. Tempany, K.H. Zou, S.G. Silverman, D.L. Brown, A.B. Kurtz, B.J. McNeil, Staging of advanced ovarian cancer: comparison of imaging modalities—report from the radiological diagnostic oncology group, *Radiology* 215 (2000) 761–767, <https://doi.org/10.1148/radiology.215.3.r00jn25761>.
- [21] E. Sala, A. Rockall, D. Rangarajan, R.A. Kubik-Huch, The role of dynamic contrast-enhanced and diffusion weighted magnetic resonance imaging in the female pelvis, *Eur. J. Radiol.* 76 (2010) 367–385, <https://doi.org/10.1016/j.ejrad.2010.01.026>.
- [22] R.N. Low, C.P. Sebrects, R.M. Barone, W. Muller, Diffusion-weighted MRI of peritoneal tumours: comparison with conventional MRI and surgical and histopathologic findings—a feasibility study, *AJR* 193 (2009) 461–470, <https://doi.org/10.2214/AJR.08.1753>.
- [23] M. Bozkurt, S. Doganay, M. Kantarci, A. Yalcin, S. Eren, S.S. Atamanalp, I. Yuce, M.I. Yildirgan, Comparison of peritoneal tumour imaging using conventional MR imaging and diffusion-weighted MR imaging with different b values, *Eur. J. Radiol.* 80 (2011) 224–228, <https://doi.org/10.1016/j.ejrad.2010.06.004>.
- [24] G. Manenti, C. Cicciò, E. Squillaci, L. Strigari, F. Calabria, R. Danieli, O. Schillaci, G. Simonetti, Role of combined DWIBS/3D-CE-T1w whole-body MRI in tumour staging: comparison with PET-CT, *Eur. J. Radiol.* 81 (2012) 1917–1925, <https://doi.org/10.1016/j.ejrad.2011.08.005>.
- [25] J.M. Winfield, N.M. deSouza, A.N. Priest, J.C. Wakefield, C. Hodgkin, S. Freeman, M.R. Orton, D.J. Collins, Modelling DW-MRI data from primary and metastatic ovarian tumours, *Eur. Radiol.* 25 (2015) 2033–2040, <https://doi.org/10.1007/s00330-014-3573-3>.
- [26] T. Takahara, Y. Imai, T. Yamashita, S. Yasuda, S. Nasu, M. Van Cauteren, Diffusion weighted whole body imaging with background body signal suppression (DWIBS): technical improvement using free breathing, STIR and high resolution 3D display, *Radiat. Med.* 22 (2004) 275–282.
- [27] K. Michielsen, I. Vergote, K. Op de beeck, F. Amant, K. Leunen, P. Moerman, C. Deroose, G. Souverijns, S. Dymarkowski, F. De Keyzer, V. Vandecaveye, Whole-body MRI with diffusion-weighted sequence for staging of patients with suspected ovarian cancer: a clinical feasibility study in comparison to CT and FDG-PET/CT, *Eur. Radiol.* 24 (2014) 889–901, <https://doi.org/10.1007/s00330-013-3083-8>.
- [28] S. Dhand, M. Thakur, R. Kerkar, P. Jagmohan, Diffusion-weighted imaging of gynecologic tumours: diagnostic pearls and potential pitfalls, *Radio Graphics* 34 (2014) 1393–1416, <https://doi.org/10.1148/rg.345130131>.
- [29] M. Torkzad, N. Casta, A. Bergman, H. Ahlström, L. Pählman, H. Mahteme, Comparison between MRI and CT in prediction of peritoneal carcinomatosis index (PCI) in patients undergoing cytoreductive surgery in relation to the experience of the radiologist: MRI and CT for prediction of PCI, *J. Surg. Oncol.* 111 (2015) 746–751, <https://doi.org/10.1002/jso.23878>.
- [30] R.N. Low, R.M. Barone, J. Lucero, Comparison of MRI and CT for predicting the peritoneal cancer index (PCI) preoperatively in patients being considered for cytoreductive surgical procedures, *Ann. Surg. Oncol.* 22 (2015) 1708–1715, <https://doi.org/10.1245/s10434-014-4041-7>.
- [31] P. De Iaco, A. Musto, L. Orazi, C. Zamagni, M. Rosati, V. Allegri, N. Cacciari, A. Al-Nahhas, D. Rubello, S. Venturoli, S. Fanti, FDG-PET/CT in advanced ovarian cancer staging: value and pitfalls in detecting lesions in different abdominal and pelvic quadrants compared with laparoscopy, *Eur. J. Radiol.* 80 (2011) e98–e103, <https://doi.org/10.1016/j.ejrad.2010.07.013>.
- [32] S. Schmidt, R.A. Meuli, C. Achteri, J.O. Prior, Peritoneal carcinomatosis in primary ovarian cancer staging: comparison between MDCT, MRI, and 18F-FDG PET/CT, *Chin. Nucl. Med.* 40 (2015) 371–377, <https://doi.org/10.1097/RLU.0000000000000768>.
- [33] R.N. Low, R.M. Barone, Combined diffusion-weighted and gadolinium-enhanced MRI can accurately predict the peritoneal cancer index preoperatively in patients being considered for cytoreductive surgical procedures, *Ann. Surg. Oncol.* 19 (2012) 1394–1401, <https://doi.org/10.1245/s10434-012-2236-3>.
- [34] M. Rosendahl, P. Harter, S.F. Bjørn, C. Høgdall, Specific regions, rather than the entire peritoneal carcinosis index, are predictive of complete resection and survival in advanced epithelial ovarian cancer, *Int. J. Gynecol. Cancer* 28 (2018) 316–322, <https://doi.org/10.1097/IGC.0000000000001173>.
- [35] K.L.M. Michielsen, I. Vergote, R. Dresen, K. Op de Beek, R. Vanslebrouck, F. Amant, K. Leunen, P. Moerman, S. Fieus, F. De Keyzer, V. Vandecaveye, Whole-body diffusion-weighted magnetic resonance imaging in the diagnosis of recurrent ovarian cancer: a clinical feasibility study, *BJR* 89 (2016) 20160468, <https://doi.org/10.1259/bjr.20160468>.
- [36] M. Espada, J.R. Garcia-Flores, M. Jimenez, E. Alvarez-Moreno, M. De Haro, L. Gonzalez-Cortijo, G. Hernandez-Cortes, V. Martinez-Vega, R. Sainz De La Cuesta, Diffusion-weighted magnetic resonance imaging evaluation of intra-abdominal sites of implants to predict likelihood of suboptimal cytoreductive surgery in patients with ovarian carcinoma, *Eur. Radiol.* 23 (2013) 2636–2642, <https://doi.org/10.1007/s00330-013-2837-7>.
- [37] J. Fehniger, S. Thomas, E. Lengyel, C. Liao, M. Tenney, A. Oto, S.D. Yamada, A prospective study evaluating diffusion weighted magnetic resonance imaging (DW-MRI) in the detection of peritoneal carcinomatosis in suspected gynecologic malignancies, *Gynecol. Oncol.* 142 (2016) 169–175, <https://doi.org/10.1016/j.ygyno.2016.04.018>.
- [38] K. Michielsen, R. Dresen, R. Vanslebrouck, F. De Keyzer, F. Amant, E. Mussen, K. Leunen, P. Berteloot, P. Moerman, I. Vergote, V. Vandecaveye, Diagnostic value of whole body diffusion-weighted MRI compared to computed tomography for pre-operative assessment of patients suspected for ovarian cancer, *Eur. J. Cancer* 83 (2017) 88–98, <https://doi.org/10.1016/j.ejca.2017.06.010>.
- [39] M.-A. Berthelin, M. Barral, C. Eveno, P. Rousset, R. Dautry, M. Pocard, P. Soyfer, A. Dohan, Preoperative assessment of splenic involvement in patients with peritoneal carcinomatosis with CT and MR imaging, *Eur. J. Radiol.* 110 (2019) 60–65, <https://doi.org/10.1016/j.ejrad.2018.11.022>.
- [40] B. Li, Q. Li, W. Nie, S. Liu, Diagnostic value of whole-body diffusion-weighted magnetic resonance imaging for detection of primary and metastatic malignancies: a meta-analysis, *Eur. J. Radiol.* 83 (2014) 338–344, <https://doi.org/10.1016/j.ejrad.2013.11.017>.
- [41] R.A. Kubik-Huch, W. Dörffler, G.K. Von Schulthess, B. Marincek, O.R. Köchli, B. Seifert, U. Haller, H.C. Steinert, Value of (18F)-FDG positron emission tomography, computed tomography, and magnetic resonance imaging in diagnosing primary and recurrent ovarian carcinoma, *Eur. Radiol.* 10 (2000) 761–767, <https://doi.org/10.1007/s003300051000>.
- [42] B. Gadelhak, A.M. Tawfik, G.A. Saleh, N.M. Batouty, D.M. Sobh, O. Hamdy, B. Refky, Extended abdominopelvic MRI versus CT at the time of adnexal mass characterization for assessing radiologic peritoneal cancer index (PCI) prior to cytoreductive surgery, *Abdom. Radiol.* 44 (2019) 2254–2261, <https://doi.org/10.1007/s00261-019-01939-y>.